Supplementary Information for the Submission "Label-free Focusing of Viral Particles under a Temperature Gradient Coupled with Continuous Swirling Flow"

Danli Luo, Chao Zhao, Guanyang Xue, Zhibo Cao, Alparslan Oztekin, Xuanhong Cheng

Mathematical Model

The profiles of velocity U, pressure p and temperature T in the microfluidic channel were simulated using the mass conservation, momentum and energy equations, respectively.

The mass conservation equation:

$$\frac{\partial \rho}{\partial t} + \nabla \cdot (\rho U) = 0 \tag{1}$$

where ρ is the density and U is the velocity.

The momentum equation:

$$\frac{\partial (\rho U)}{\partial t} + \nabla \cdot (\rho U \otimes U) - \nabla \cdot (\mu \nabla U) = -\nabla p + \rho g \tag{2}$$

Where $\otimes$ is the tensor product, p is the pressure, μ is the dynamic viscosity, and g is the gravitational acceleration.

The energy equation:

$$\frac{\partial (\rho e)}{\partial t} + \nabla \cdot (\rho U e) + \frac{\partial (\rho K)}{\partial t} + \nabla \cdot (\rho U K) = \nabla \cdot \left(\frac{\kappa}{c_p} \nabla e \right) + \rho U \cdot g - \nabla \cdot (pU) \tag{3}$$

where e is the internal energy density, $K = |U|^2/2$ is the kinetic energy density, κ is the thermal conductivity and c_p is the specific heat.

The dimensionless concentration C was solved by the transient mass transport equation with an additional thermophoresis term:

$$\frac{\partial c}{\partial t} + \nabla \cdot (Uc) = \nabla \cdot (D S_T \nabla T c) + \nabla \cdot (D \nabla c) \tag{4}$$

where c is the concentration, S_T is the Soret coefficient and D is the diffusion coefficient. The input concentration is uniform and defined as one.

The diffusion coefficient was evaluated by the Stokes-Einstein equation:

$$D = \frac{k_B T}{3\pi \mu d} \tag{5}$$

Where k_B is Boltzmann constant and d is the particle diameter.

The average concentration $\bar{c}$ was evaluated by the surface integral ratio of mass flux to volume flux:

$$\bar{c} = \frac{\int_{c.s.} cU \cdot \vec{n} ds}{\int_{c.s.} U \cdot \vec{n} ds} \tag{6}$$

Where $c.s.$ is the designated cross-sectional area and $\vec{n}$ is the surface normal vector.

Soret coefficients

Table S1. Values of the Soret coefficient used in simulations against particle diameter and species. S_T values of four sizes of polystyrene particles, $25, 50, 100, \text{and } 1000 \text{ nm}$, were experimentally measured and found to follow a power function with an exponent of ~1.45. This dependence is consistent with the literature[1] and was used to interpolate S_T of polystyrene particles of other diameters.

Particle Species	Diameter (nm)	Soret Coefficient (1/K)	Data Source
Polystyrene	25 nm	0.0325	Experiment[2]
	50 nm	0.0887	Experiment[2]
	100 nm	0.2250	Experiment[2]
	200 nm	0.6587	Interpolation
	300 nm	1.1840	Interpolation
	400 nm	1.7950	Interpolation
	1000 nm	6.7400	Experiment[2]
HIV virus		0.1700	Experiment[2]

Simulation of the temperature profile

To analyze the temperature distribution in the microfluidic device, the device assembly was simulated in ANSYS Fluent. The mesh of each layer (**Fig. S1a**) was generated separately and coupled at the interfaces for heat transfer. The temperature distribution (**Fig. S1b**) from the heat transfer simulation was extracted, and the temperature at the interfaces was applied as the boundary condition for the flow and mass transport simulations.

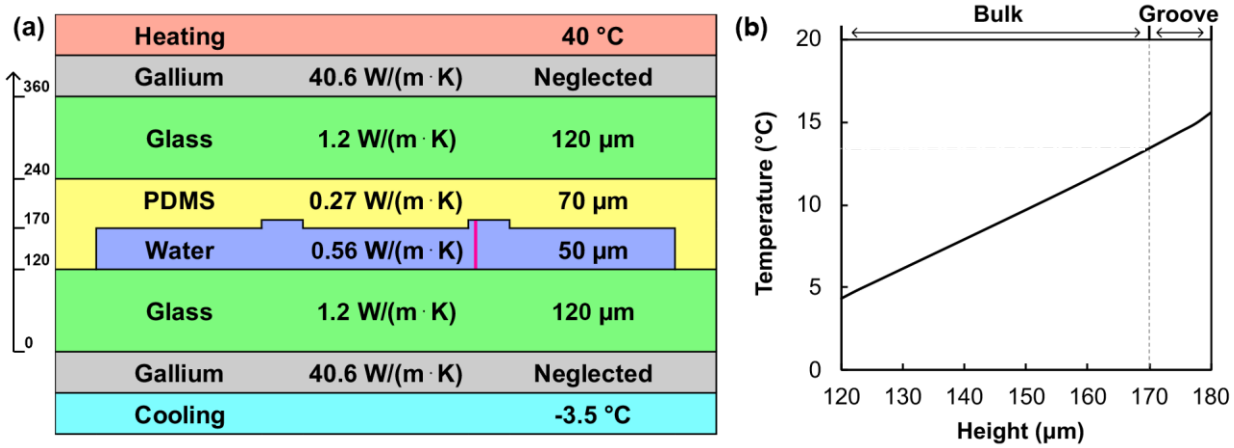

Figure S1. (a) The multi-region structure used in the heat transfer model to estimate temperature distribution. The grooves in the water layer have a height of $10\ \mu m$. (b) The steady-state temperature profile across the water layer (red vertical line in the left panel) from numerical analysis. A $12\ ℃$ temperature difference, $4\ ℃ - 16\ ℃$, is established in the water layer (including the groove region), roughly 28% of the temperature drop applied over the entire device.

The computational domain in the flow and mass transport simulations only contains the water-filled volume in **Fig. S1a**. The mesh was generated using the Cutcell method in ANSYS. To avoid divergence in unstructured meshes, $5\mu m$ hexahedral mesh cells were used in the bulk region. The groove and corner regions were refined to $2.5\mu m$ to capture the flow vortices and concentration gradient (**Fig S2**). The ANSYS mesh was then converted to the OpenFOAM format and extended to $32cm$.

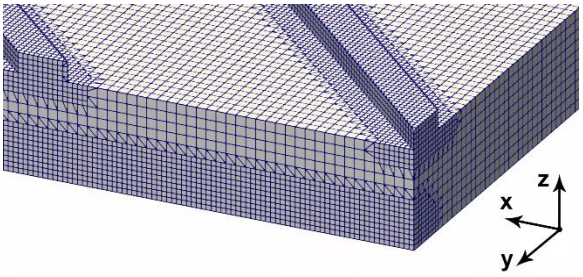

Figure S2. A portion of the mesh used in the numerical simulation. The sample fluid flows along the positive x-direction. The bulk region uses $5\mu m$ hexahedral cells. The groove region' mesh is $45°$ angled, and the concentration corners have been refined to $2.5\mu m$.

Simulation of the concentration and mass flux

Two different approaches were used in the concentration distribution analysis. First, the cross-sectional concentration contours were directly compared against confocal images. On the other hand, the averaged outlet concentration was evaluated as the integral of the mass flux. As the mass flux represents the amount of mass passing through the cross-sectional surface per unit time and unit area, it was calculated by integrating the product of concentration and axial velocity (**Fig. S3**). Thus the integral of the mass flux over the Outlet 1 area represents the total mass flow rate of Outlet 1.

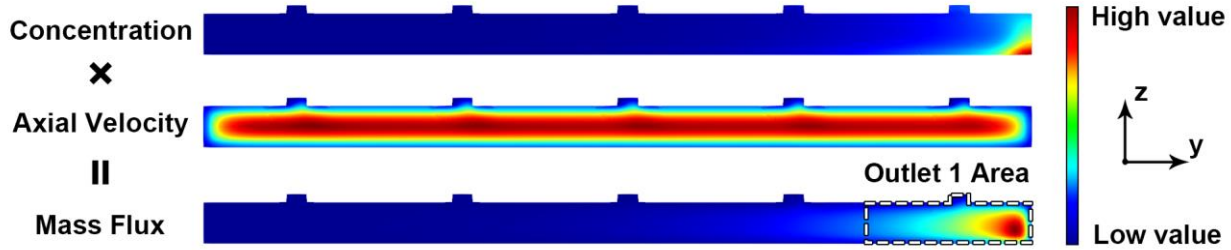

Figure S3. Simulated cross-sectional images of the concentration, axial velocity, and mass flux near the outlet. Mass flux is the product of concentration and axial velocity. The axial velocity points at the positive x-direction and perpendicular to the cross-sectional surface. The area corresponding to Outlet 1 is enclosed with dashed lines in the Mass Flux panel. The average mass flux was calculated from Equation (6).

Span-wise velocity in the microfluidic device

Confocal microscopy was employed here to characterize lateral transport of $100\ \mathrm{nm}$ polystyrene particles in microchannels with or without microgrooves on the channel floor. The particles and water were flowed into the microfluidic device side by side. In the flat bed channel (**Fig. S4a**), nanoparticles diffused sideways as they were carried by the axial flow, leading to a diffusive interface. On the other hand, with grooves on the channel floor (**Fig. S4b**), nanoparticles migrated rapidly in the lateral direction and preferentially along the groove side, indicating additional transport by the transverse flow. Here the main channel width (W) is $500\ \mu\mathrm{m}$, height (H) is $50\ \mu\mathrm{m}$, groove width (w) is $50\ \mu\mathrm{m}$, height (h) is $10\ \mu\mathrm{m}$, spacing (s) is $50\ \mu m$, and tilting angle (θ) is $45°$. The average axial velocity is $1\ \mathrm{mm/s}$. The transverse flow promotes nanoparticle enrichment in the presence of an orthogonal temperature gradient. The transverse velocity is found proportional to the sample flow rate by flow simulation (**Fig. S4c**).

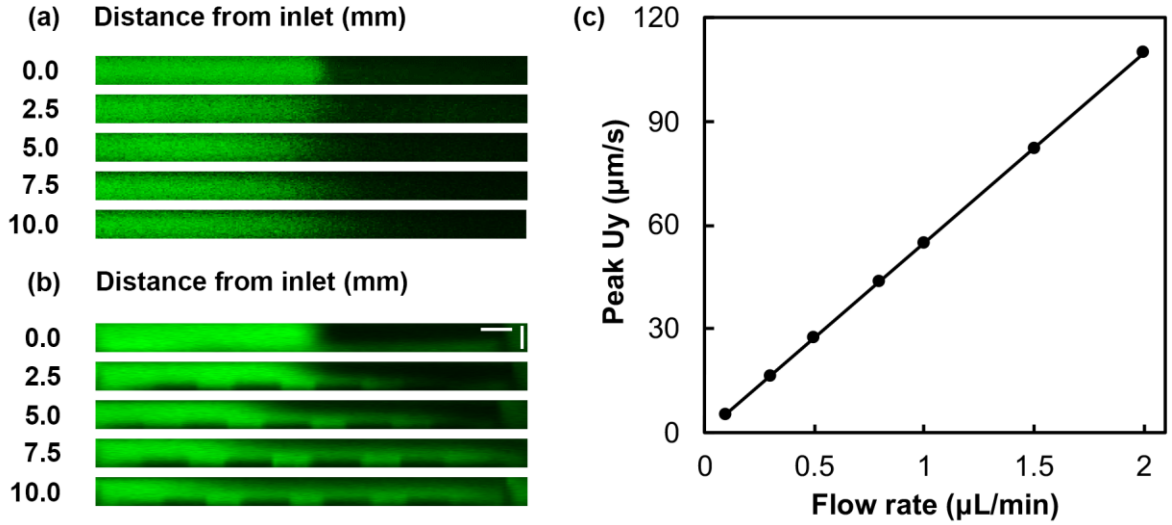

Figure S4. Confocal microscopic cross-sectional images were taken across (a) a flat channel and (b) a grooved channel at room temperature. Polystyrene particles $100\ nm$ in diameter and at a concentration of 0.1% was injected into the microfluidic channel side by side with water. The distance from a bifurcated inlet is marked on the left. While nanoparticles diffuse to the waterside in the flat channel, a span-wise sweep of the nanoparticles is observed in the device with the grooves. Both scale bars represent $50\mu\mathrm{m}$. (c) The peak magnitude of the transverse velocity U_y as a function of sample flow rates.

References

1 Andreev, A. F. Thermophoresis in liquids. *Zhurnal Eksperimentalnoi i Teoreticheskoi Fiziki* **94**, 210 (1988).

2 Zhao, C. *Microfluidic Nanoparticles Focusing and Separation,* PhD thesis, Lehigh University, available at https://preserve.lehigh.edu/etd/2907 (2015).